

**Biogeochemical Processes in a Clay Formation In-situ Experiment:  
Part B – Results from overcoring and evidence of strong buffering by the  
rock formation**

**M. Koroleva<sup>1,3</sup>, C. Lerouge<sup>2</sup>, U. Mäder<sup>1\*</sup>, F. Claret<sup>2</sup>, E. Gaucher<sup>2</sup>**

<sup>1</sup> Institute of Geological Sciences, University of Bern, Baltzerstrasse 3, CH-3012 Bern,  
Switzerland

<sup>2</sup> BRGM, French Geological Survey, 3 avenue Claude Guillemin, B.P. 36009, 45060 Orléans  
Cedex 2, France

<sup>3</sup> Present address: Geologisch-Paläontologisches Institut, Universität Hamburg, Bundesstrasse  
55, D-20146 Hamburg, Germany

---

\* Institute of Geological Sciences  
University of Bern  
Baltzerstrasse 3  
CH-3012 Bern, Switzerland  
E-mail: urs.maeder@geo.unibe.ch  
Tel: +41 31 631 87 61  
Fax: +41 31 631 48 43

## Abstract

An in-situ Porewater Chemistry (PC) experiment in the Opalinus Clay formation was carried out at the Mont Terri underground rock laboratory (Jura Mountains, Switzerland) for a period of five years. A traced water with a composition close to that expected in the formation was continuously circulated and monitored in a packed-off borehole to achieve diffusive equilibration. An unwanted microbial perturbation changed the water composition, characterized by reduction of sulphate combined with increasing sulphide, increasing alkalinity, decreasing pH and increasing  $P(\text{CO}_2)$ . In contrast, the main cations (Na, Ca, Mg) remained remarkably constant during the experiment, thus indicating the strong buffering of the formation via cation and proton exchange as well as carbonate dissolution/precipitation reactions.

After five years, the 4.5 m long vertical test interval was overcored and Opalinus clay samples were analyzed along ca. 15 cm long radial profiles. The analytical investigations included mineralogy (XRD, SEM-EDX), bulk parameters (water content, density, C, S), cation exchange capacity and occupancy, aqueous leachates for  $\text{Cl}^-$ ,  $\text{Br}^-$ ,  $\text{SO}_4^{2-}$  and water and carbonate stable isotopes. Emphasis was put on best sample preparation and conservation techniques.

Results show that the distribution of non-reactive tracers ( $\text{Br}^-$  and  $^2\text{H}$ ) follows the expected out/in-diffusion profiles compatible with the time-dependent boundary conditions in the test interval of the borehole. Although some experimental features remain unresolved (e.g. high content of leachable sulphate compared to test interval), the distribution of reactive tracers (in porewater, on the clay exchanger and in the solid phase) demonstrate the very extensive buffer capacity of the Opalinus Clay formation towards chemical disturbances, such as those induced by microbial sulfate reduction and oxidation of an organic carbon source.

**Key words:** clay formation, microbial perturbation, Opalinus Clay, Mont Terri, buffering

## 1. Introduction

Argillaceous formations are being considered as potential host rocks for the deep geological disposal of radioactive waste due to their low permeability and large sorption capacity. Diffusion properties and reactive transport have been examined with in-situ experiments at the Mont Terri Rock Laboratory for more than 10 years (Pearson et al., 2003; Soler et al., 2008; Wersin et al., 2009). The Porewater Chemistry (PC) Experiment was a five-year diffusion experiment (2002-2007) carried out in a 4.5 m long test interval that crossed also a zone containing fault rocks, and it was equipped with a fluid circulation system. Details of the set-up and geochemical evolution of the test water is described by Wersin et al. (2010a; this issue).

The experiment initially aimed at constraining in-situ pore water conditions, but microbial activity perturbed the chemical system, and the characterization and understanding of the perturbation and its effects then became a main focus (Stroes-Gascoyne et al., 2010; this issue; Tournassat et al., 2010; this issue; Wersin et al., 2010b; this issue). The objective of the overcoring was to examine the extent to which the Opalinus Clay surrounding the test interval responded to the complex geochemical evolution of the fluid composition within the test interval.

The sampling strategy was to excavate the entire test interval by overcoring and subsample along radial profiles at different depths. Apart from mineralogy, geochemistry and physical properties, also information to constrain pore water chemistry was thought, namely by aqueous leaching and the determination of cation exchange capacity and selectivity, as well as stable isotope composition determined by different methods.

## 2. Initial and boundary conditions of the in-situ experiment

A full description of the experiment is provided by Wersin et al. (2010a; this issue). Here, we summarize the key parameters relevant for the understanding and interpretation of

the analytical results from the samples obtained from overcoring. Artificial pore water was circulated for five years with a composition to match the expected major components of the in-situ pore water. A gas mixture was used in the head space of the circulation reservoir to prescribe a partial pressure of CO<sub>2</sub> of 10<sup>-3.5</sup> bar. Bromide and deuterium were used as tracers to observe a loss over time to the formation by diffusion.

Sulphate reducing bacteria became active and this led to a marked decrease of sulphate concentrations over time (Table 1). A contamination by organic carbon (glycerol and possibly minor acetone; De Cannière et al., 2010: this issue) and graphite electrodes occurred initially, and this led to the production of inorganic carbon by bacterial activity (oxidation of organic carbon and reduction of sulphate). The pH decreased over time to a value of ~6.7 while sulphate concentration decreased, and sulphide and alkalinity increased due to bacterial sulphate reduction. The full data set is included in Wersin et al. (2010a; this issue).

The test interval was sampled and emptied 16 days before overcoring, and a slight argon overpressure was shut in (Table 1, and analyses in Wersin et al., 2010a; this issue). There was a strong smell of H<sub>2</sub>S, and in-line filtration was performed to sample suspended black material. The interval was emptied again before the pressure had to be released followed by cutting fluid lines for preparing overcoring one week before recovering the first core segment. Some in-flow to the interval occurred during this last week, and some of this water was recovered with the deepest core segment containing the end of the test interval.

### **3. Overcoring and sample material**

#### Overcoring

The 4.5 m long vertical test interval at 5.5-10 m depth consisted of a segmented porous polyethylene hollow cylinder (50 mm OD, 30 mm ID) with a solid PVC core, topped by a mechanical packer, and a service tube for flow lines to the surface (Fig. 1). The annular space between the service tube and the claystone was filled with epoxy resin to provide a

permanent seal. Overcoring was initially not foreseen and a borehole survey was not performed.

A 200 mm diameter borehole was first drilled off-centre along the service tube in order to cut the equipment at depth with a down-hole side cutter above the packer (Fig. 1). This borehole was back-filled with mortar, and the service tube was overcored and removed. Powdered claystone and epoxy resin were used to stabilise and seal the top of the cut equipment.

The overcoring equipment employed was an adaptation of a heavy triple-barrel equipment used at the Grimsel Test Site (<http://www.grimsel.com/>) for granite, with a 386 mm outer diameter and a 284 mm core diameter. The second (inner) barrel was suspended from the cross-over at the top to ensure rotation-free conditions. Inside this second barrel, a heavy-walled segmented acrylic liner was placed to further protect the core. This liner was simply slid over the core as drilling progressed, and the liner was staying on the core during extraction and handling of core segments. The adaptation from previous applications at the Grimsel Test Site included conversion to air-cooled dry drilling and the ability to retrieve an overcore of 5.5 m length in a single core pull, i.e. the entire test interval.

Drilling to 5.3 m depth was carried out on April 26, 2007. Unfortunately, the top part of the equipment (packer, topmost filter cylinder, central PVC tube) was pulled out with the overlying core. The borehole was flooded with argon, and the packer re-installed at depth to protect the test interval. Overcoring started the following day, but came to a halt when penetrating the fault zone ("Main Fault") due to extra moisture contained in the fault rock and resultant clogging of the core and barrels. The top half of the interval (5.3-7.4 m) was retrieved, but the fault section (7.4-9 m) was lost (ground and exhausted). The bottom part (9-10.5 m) was cored and recovered the following morning.

The filter section was well preserved from 6.5-7 m, but completely mashed towards the fault section below due to the afore mentioned drilling difficulties. Filters were well

preserved in the lower core. Argon flushing was provided during idle time, and also during core recovery. The core segments were left in the acrylic liners, sealed off with caps, and preserved under argon until further handling.

#### Profile locations and Sampling procedures

Three radial profiles (A, B and C) were sampled from oval segments which were collected from different depth levels parallel to bedding (Fig. 2). Profile A was taken from a depth of 6.6 m by BRGM, profiles B and C were collected by the University of Bern from a depth of 6.7 and 9.7 m.

Downsizing of the large overcore segments (>100 kg) preserved in their acrylic liners was performed by a combination of cutting with a large low-speed mechanical whip saw, and cleaving along bedding planes or bedding-parallel fracture planes. Argon flushing and wrapping with tin foil or plastic film was employed during cutting to minimize drying and exposure to atmosphere. Subsamples were then transported in plastic wraps to an adjacent processing site equipped with a band saw, cleaving tools, vacuum-sealing equipment and liquid nitrogen for further sub-sampling and sample preservation. Special care was taken for samples intended for microbiological studies, by disinfecting cutting equipment and core liners with burning alcohol, wearing breathing masks, and using filters for argon flushing.

The segment for radial profile A was divided into two parts with sample storage adapted to the analysis type. For the aqueous leaching measurements, half of the segment was cut and immediately stored in liquid nitrogen until transfer into a glove box (<1 ppm O<sub>2</sub> atmosphere) at the BRGM laboratory in order to avoid any oxygen contamination. For the mineralogical characterization, the equivalent half part of the segment was stored in plasticized aluminium bags sealed under vacuum and previously purged under argon atmosphere. Black "slimy" material was scraped off the borehole wall and also preserved by sealing in vacuum.

Samples from radial profiles B and C were dry cut using a small band saw (Fig. ). Afterwards, the sub-samples were divided into 4 pieces each: (1) for aqueous and Ni-en extraction tests, (2) for bulk density measurements, (3) for water isotope determinations, and (4) for gravimetric water content measurements. Each sub-sample was moderately evacuated and sealed in a thick-walled plastic bag. Each plastic bag was inserted into a plasticized aluminium bag, which was again evacuated and then sealed. The initial wet mass of the samples required for gravimetric water content was determined immediately after sampling. The samples for pore water investigations were further processed in the laboratory after 2-3 days of cold storage.

Small samples from the residual borehole fluid that accumulated in the bottom core sample were taken by BRGM for analysis of black suspended material, and these were preserved by sealing in vacuum. Observations on a filter residue taken during the final interval sampling campaign are also included in this report. This sample was obtained by in-line filtration during sampling, and preservation of the filter cartridge by evacuation and sealing in plastic. The sample was analyzed within a few days at the University of Bern prior to overcoring.

## **4. Methods**

### *4.1. Mineralogical characterization*

X-ray diffraction (XRD) measurements were performed on profile A sub-samples with a SIEMENS D5000 X-ray diffractometer with Co  $K\alpha_{1+2}$  radiation operating at 40 kV and 100 mA, and on profile B sub-samples with a Philips PW 1800 diffractometer. The complete mineralogy was obtained by XRD measurement of bulk-rock powder, whereas the clay fraction was determined by XRD of oriented samples of the  $<2\mu\text{m}$  fraction that were air-dried, saturated with ethylene glycol, and heated at 550°C. Mineral identification was performed using standard X-ray diffraction libraries. Mineral quantification from X-ray

patterns was performed on samples of profile B using laboratory internal standardisation. The content of sheet silicates (clay minerals) was calculated by difference: total clay = 100wt.% -  $\sum$  wt.% (quartz, feldspars, carbonates, pyrite, C<sub>org</sub>).

The contents of total sulphur, total carbon and inorganic carbon were determined in samples from profiles B and C with a CS-mat 5500 element analyzer (Ströhlein GmbH, Germany). The carbonate contents were determined in the samples from profile A using the calcimetry method NF P 94-048 with a BERNARD calcimeter. The carbonate contents (calcite, dolomite and siderite) for profile B and C were calculated from the inorganic carbon content combined with the XRD data. The pyrite content was calculated from the total sulphur content assuming that pyrite is the only S-bearing phase.

Scanning electron microscope (SEM) observations, EDX analyses and elemental mapping were performed with a JEOL JSM 6100 instrument coupled with an energy-dispersive spectrometer (Kevex Quantum) operated at 25 kV at BRGM. Prior to analysis, a thin carbon layer was sputter-coated on the samples (Edwards Auto 306). SEM analyses at the university of Bern were performed on uncoated samples in low vacuum (10 Pa) with a Zeiss EVO50 XVP instrument, operated at 20 keV and a beam current of 100-1400 nA for EDX analysis (EDAX Sapphire light element detector).

Transmission electron microscope (TEM) observations and analyses were performed at the Orléans University on a Philips CM20 with a CCD Gatan camera, at 200 kV. The TEM samples were prepared by dispersing powdered samples in alcohol by ultrasonic treatment, dropping them onto a porous carbon film supported on a copper grid, and then drying them in air.

Electron microprobe chemical analyses were performed using a Camebax SX50 instrument and ZAF correction. Analyses of silicates and carbonates were performed with 15 kV acceleration voltage, a beam current of 12 nA and a 1-2  $\mu$ m beam width. Analyses of sulphides were performed with 20 kV acceleration voltage and 20 nA. Counting time was 10 s

for major elements and 20 s for trace elements. Standards used included both well-characterized natural minerals and synthetic oxides.

#### *4.2. Water content and bulk density*

The water content was determined by drying sample aliquots of approximately 17 to 52 g to constant mass at 105°C. The bulk wet densities were determined by the Paraffin oil displacement method. From these quantities the water-loss porosity and bulk dry density were calculated (Pearson et al., 2003; Gimmi, 2003; Nagra, 2002).

The water content is also obtained from the isotope diffusive-exchange method (Rübel et al., 2002), but is of lesser accuracy and it is used as a consistency test for the isotope determinations (see below).

#### *4.3. Aqueous leaching and cation exchange properties*

An aqueous extraction was performed to quantify the amounts of soluble salts present in the rock. All extraction tests were conducted under oxygen-free atmosphere in order to minimise pyrite oxidation.

The powdered sub-samples of profile A were leached with deionised water that was boiled and degassed. Extraction tests were performed at a solid:liquid ratio of 0.001, 0.01, 0.1, and 1 (kg rock per kg water) during 10 min and 24 hours. After the leaching procedure, the liquid was filtered at 0.1µm prior to analysis. Chloride, bromide and sulphate concentration were measured by ion chromatography. Dissolved organic and inorganic carbon were measured using a Shimadzu TOC carbon analyser.

The sub-samples of profile B were dried prior the aqueous extraction and cation occupancy determinations, followed by crushing by hand to a grain size of approx. 5 mm in order to minimise possible contributions from fluid inclusions. Drying and crushing were conducted under N<sub>2</sub> atmosphere inside a glove box at room temperature. Extraction tests were

performed at solid:liquid ratios of 0.1, 0.25, 0.5 and 1 (kg rock per kg water) using deionised oxygen-free water that was prepared in a glove box by N<sub>2</sub> bubbling during 30 min. Each sample was shaken end-over-end for 7 days in polypropylene tubes in order to equilibrate the extract solution with calcite and dolomite of the rock (Bardbury and Baeyens, 1998; Pearson et al., 2003). After filtration (0.45 µm) the supernatant solutions were immediately analysed for pH and alkalinity by titration. Anions and cations in the extract solutions were analysed by ion chromatography with a Metrohm 861 Compact IC-system.

Cation exchange capacity (CEC) and cation occupancies were determined by displacement with nickel ethylenediamine (Ni-en) (Bradbury and Baeyens, 1998). This displacement was carried out using 30 g of rock powder at solid:liquid ratios (S:L) of 0.25, 0.5, 1.0, 1.5 (kg rock per kg solution) using deionised oxygen-free water that was prepared in a glove box. Each sample was shaken end-over-end for 7 days under N<sub>2</sub> atmosphere inside a glove box. After solid separation by centrifugation, the supernatant leachate was filtered to <0.45 µm. Analyses including Na, K, Ca, Mg, Sr and Ni were performed using atomic adsorption spectrometry.

#### *4.4. Stable isotope ratios of carbonates and pore water*

Calcite was extracted by an acid attack with phosphoric acid (100% anhydrous) at a temperature of 70°C during 3 minutes on an automated line (“carbo device”) coupled with a Finnigan Mat delta S mass spectrometer for determining δ<sup>13</sup>C and δ<sup>18</sup>O. The fractionation coefficient used for the calculations is from Swart et al. (1991). The results are reported in δ units relative to international standards VSMOW for oxygen and PDB for carbon. The reproducibility was ±0.2‰ for oxygen and carbon.

The stable isotopic composition of pore water was determined using the diffusive-exchange technique (Rübel et al., 2002). The method is based on diffusive exchange via the

vapour phase between the preserved pore water of a rock sample and two different test waters of known but contrasting isotopic composition in a sealed container at room temperature.

Saturated rock pieces from the radial profiles B and C of approximately 2 cm in size (200-300 g) were placed in a vapour-tight container together with a small crystal dish containing a known mass of test water with known isotopic composition. The two different test waters used are de-ionized laboratory water (LAB) and glacial melt water (SSI). In order to prevent mass transfers and isotope fractionation (e.g., Horita et al., 1993a, 1993b) between the test water and the pore water of the rock through desiccation-condensation mechanisms, the water activity of the test water must be adjusted to fit the water activity in the rock samples, which depends on the type and concentration of salts, and on the proportion of water bound to the mineral surfaces (Sposito, 1990). Therefore, 0.3 M NaCl was added to the test water to match the water activity of 0.98, a typical value for the Opalinus Clay. The three-reservoir system (rock sample, test water and the air inside the container) was equilibrated for 30 days at room temperature in order to achieve complete isotope equilibrium (Rübel et al., 2002). After equilibration, the test water was removed from the crystallisation dish and analysed by IRMS at the Hydroisotop GmbH laboratory. The rock material was dried in an oven to constant mass at 105°C in order to obtain the gravimetric water loss of the samples. The error of the equilibration experiment was calculated applying Gaussian error propagation.

The observed shift of the isotopic compositions of the test waters allows the calculation of the isotopic composition of the pore water. The water contents of the samples used in the LAB and SSI experiments are identical, and the  $\delta^{18}\text{O}$  and  $\delta^2\text{H}$  of the pore water is calculated according to:

$$c_{pw(t=0)} = \frac{m_{twLAB}c_{twSSI(t=\infty)}m_{rockSSI}(c_{twLAB(t=\infty)} - c_{twLAB(t=0)}) - m_{twSSI}m_{rockLAB}c_{twLAB(t=\infty)}(c_{twSSI(t=\infty)} - c_{twSSI(t=0)})}{m_{rockSSI}(m_{twLAB}c_{twLAB(t=\infty)} - m_{twLAB}c_{twLAB(t=0)}) - m_{rockLAB}(m_{twSSI}c_{twSSI(t=\infty)} - m_{twSSI}c_{twSSI(t=0)})} \quad (1)$$

where  $m_{pw}$  and  $m_{tw}$  are the masses of pore water and test water,  $m_{rock}$  is the mass of the rock sample,  $c_{pw}$  is the original (in situ) isotopic composition of pore water, and  $c_{tw}$  is the isotopic composition of the test water at the beginning ( $t=0$ ) and at the end ( $t=\infty$ ) of the equilibration with LAB or SSI test water.

The initial  $\delta^{18}\text{O}$  or  $\delta^2\text{H}$  values in pore water in the experiments LAB and SSI are identical, and therefore, the water content is found according to:

$$WC = \frac{(c_{tw(t=\infty)SSI} - c_{tw(t=0)SSI})m_{twSSI}m_{rockLAB} - (c_{tw(t=\infty)LAB} - c_{tw(t=0)LAB})m_{twLAB}m_{rockSSI}}{m_{rockLAB}m_{rockSSI}(c_{tw(t=\infty)LAB} - c_{tw(t=\infty)SSI})} \quad (2)$$

This value can be compared to the directly measured water content as an independent check of the success of the experiment.

## 5. Results

### 5.1. Mineral characterization of the Opalinus Clay close to the water/rock interface

The total clay fraction in the profile B is quite homogeneous, ranging from 66 to 67 wt %. It is composed of illite (25-35 %), illite/smectite mixed-layers (12-14 %), chlorite (5-9 %), and kaolinite (13-20 %), without any systematic trend related to the distance of the interface to the test interval (data reported in Koroleva and Mäder, 2008).

The carbonate fractions obtained for both profiles, A and B, are comparable. They consist of calcite (12-14 %) with minor siderite (~3 %) and dolomite (< 2 %). The variations of calcite content along both profiles are small and reflect the heterogeneity of the rock (Fig. ). Carbonates occur as a detrital fraction (calcitic and aragonitic bioclasts), micritic calcite and rare euhedral calcite grains, whereas siderite and dolomite occur as disseminated 10-50 $\mu\text{m}$ -sized euhedral grains.

Pyrite is the only observed sulphur-bearing phase, occurring as disseminated framboids and clusters of framboids in all samples. Pyrite content ranges between 1.5 and 1.7 wt. %.

Microscopic observations of polished thin sections and bulk rock EDX spectra using SEM do not show significant mineralogical, textural and chemical variations along all radial profiles. This is consistent with previous data obtained for Opalinus Clay (Pearson et al., 2003).

Elemental mapping of major elements, which was performed adjacent to the water/rock interface (within 300  $\mu\text{m}$ ), also shows no significant changes in chemical and mineralogical composition (Fig. ). Framboidal pyrite present in the Opalinus clay formation remained stable at the water/rock interface (Fig. 5a). Euhedral grains of carbonate close to the water/rock interface do not exhibit any dissolution or growth features on surfaces (Fig. 5b, c). Calcite was observed as micro-coating on the wall of the PC-borehole, suggesting a precipitation of calcite at the water/rock interface (Fig. ). Gypsum was also identified at the interface, whereas it is absent further away from the interface. Complementary TEM observations on particles leached by alcohol from the subsample close to the PC-borehole wall confirmed the neo-formation of carbonates, and provided evidence of an S-bearing phase and euhedral small Ca-phosphates. Although samples were preserved in liquid nitrogen until examination in order to preserve redox conditions, a possible rapid oxidation of labile sulfides into gypsum during preparation of the sample cannot be excluded. Small changes in rock texture with disorientation of clay minerals and occurrence of micro-porosity were observed close to water/rock interface ( $<300 \mu\text{m}$  from the border) (Fig. 5d, e). Calcite neo-formation was also observed in the microporosity (Fig. 5f). It was impossible to determine the origin of the microporosity. It could be an artifact due to mechanical damages induced by drilling the PC-borehole and subsequent convergence, or it could also be due to limited mineral dissolution.

## 5.2. Mineral characterization of mud and precipitates formed in the borehole fluid

Comparison of X-ray diffraction results from mud collected from the test borehole with those obtained on Profile A shows that the mineralogy of the mud is quite similar to the Opalinus Clay but indicates a slightly higher carbonate content in the mud (Fig. 6).

Precipitates were also observed in the water sample taken from the bottom of the borehole. The precipitates were deposited on a thin section, covered with carbon coating and directly observed and analysed under vacuum to minimize oxidation processes. SEM observations, EDX spectra combined with EPMA analyses of the precipitates provide evidence of two major sulphide phases with different Fe/S ratios (Fig. a, b): (a) a dominant sulphide phase characterized by a Fe/S ratio close to 1, comparable to greigite ( $\text{Fe}_3\text{S}_4$ ), and (b) a sulphide phase characterized by a Fe/S ratio close to 0.5 and containing invariably Na, independent of chloride content. This latter phase could correspond to pyrite mixed with sodium salts. Sulphate particles are less common (Fig. c). They consist of Na and Na-Ca sulphate occurring as platy grains and elongate flakes, respectively. The mixing of Fe-S phases with salts renders analysis difficult. The sulphate phases are suspected to have formed during core recovery, storage and sample preparation due to oxidation of the labile sulphides, because the pore water itself is undersaturated with respect to gypsum.

Similar observations were made on black filter residue obtained during the final sampling campaign prior to overcoring; it consisted of a mixture of salts from drying, and Fe-S phases. Some very small cubes of suspected pyrite were observed. In contrast to the sample described above, the filter residue contained abundant biofilm. Other samples preserved in vacuum turned brown after a couple of weeks owing to some oxygen diffusion and the labile nature of the different Fe-sulphide phases.

In summary, combined observations and analyses indicate substantial precipitation of iron sulphide phases and minor calcite in the test interval, but no significant changes in the wall-rock adjacent to the test interval.

### 5.3. Water content and density

The average water content relative to its dry and wet mass obtained by drying at 105°C varies in the range of 8.02-8.40 wt% and 7.42-7.75 wt%, respectively. The absolute uncertainty between duplicate samples is less than 0.07 wt%. Water contents calculated by the isotope diffusive-exchange range between 9 and 12 wt% and are higher than those obtained by drying the same samples after the experiment at 105°C. For profile B they range between 9 and 12 wt% and for profile C between 8 and 15 wt%. Previous studies of the Opalinus Clay explained such differences of about 10% to 20% by possible isotopic exchange with bound water on the clay surfaces that may differ in its isotopic composition from that of the capillary water (Rübel et al., 2002).

The bulk wet density varies between 2.38 and 2.40 g/cm<sup>3</sup>. The water-loss porosity (or volumetric water content,  $\phi_{WL}$ ) can be calculated according to:

$$\phi_{WL} = WC_{wet} \rho_{b,wet} / \rho_{water}, \quad (3)$$

where  $WC_{wet}$  is water-loss relative to its wet mass,  $\rho_{b,wet}$  is bulk wet density and  $\rho_{water}$  is the density of water. Commonly, the density of pore-water of the Opalinus Clay at Mont Terri is taken as 1.00 g/cm<sup>3</sup> (Pearson et al., 2003) because the salinity of the pore water is distinctly less than that of seawater.

The water-loss porosities vary between 17.8 and 18.6 vol%. Bulk dry density can be calculated from water content and bulk wet density. The bulk dry densities vary in the range of 2.20-2.22 g/cm<sup>3</sup>. Assuming that the samples were fully saturated, the water-loss porosity value is equal to the total porosity, and the grain density can be estimated to approximately 2.71 g/cm<sup>3</sup> in agreement with previous measurements (Pearson et al., 2003).

The water contents relative to the dry mass and the bulk dry densities as function of the distance to the water/rock interface do not vary significantly along radial profiles (Fig. 8).

#### 5.4. Anion contents in aqueous leachates

The composition of an aqueous extract solution represents the sum of: (a) the constituents originally dissolved in the pore water, (b) the mineral components dissolving during the leaching process, (c) any constituents contributed from cracked fluid inclusions, and (d) effects of cation-exchange with the exchanger population of expandable clays. Aqueous extractions (profile A and B) were performed at different solid:liquid (S:L) ratios, and for profile A also at different contact times (10 min and 24 hours), in order to control the possible effect of celestite dissolution.

Cl<sup>-</sup>, Br<sup>-</sup> and SO<sub>4</sub><sup>2-</sup> concentrations are given in Table 2 in mmol/kg<sub>rock</sub>. No variation is observed as a function of different S:L ratios for these three elements. Assuming that all Cl<sup>-</sup>, Br<sup>-</sup> and SO<sub>4</sub><sup>2-</sup> leached in the aqueous extracts originates from pore water, anion concentrations in pore water can be calculated from the aqueous leaching data, grain density and the geochemical porosity using

$$A_{\text{porewater}} = \frac{A_{b,\text{rock}} \rho_{b,\text{wet}}}{\phi_A} \quad (4)$$

where  $A_{b,\text{rock}}$  is the anion concentration in mmol/kg<sub>rock</sub> (based on aqueous leaching),  $A_{\text{pore water}}$  is the anion concentration in mmol/kg<sub>H<sub>2</sub>O</sub> in pore water,  $\rho_{b,\text{wet}}$  is the bulk wet density, and  $\phi_A$  is the anion-accessible porosity.

Cl and Br concentrations (Fig. 9) and SO<sub>4</sub><sup>2-</sup> concentrations (Fig. 10) in pore water recalculated from aqueous extracts were reported as a function of the radial distance away from the test interval. Br in pore water decreases toward the outer rim, while Cl is almost constant within uncertainties. SO<sub>4</sub><sup>2-</sup> in porewater increases toward the outer rim of the profile.

### 5.5. Cation exchange capacity and cation site occupancy

The CEC is determined from the consumption of a highly selective cation (Ni) onto the exchanger and also as the sum of cations displaced from the exchange sites into solution. The measured cation concentrations (Table 3) represent the sum of cations displaced from mineral surfaces, the dissolution of salts precipitated from pore water during desiccation of the samples, and a minor contribution from the dissolution of sparsely soluble minerals, such as carbonates. Therefore, the derivation of the in-situ cation exchange population requires a correction of the measured cation concentration in the Ni-en extract with the cation contribution from the pore water. The aqueous extracts are affected by ion exchange and mineral dissolution, and therefore, some assumptions have to be made for correcting the Ni-en data since the pore water composition is not known a priori. Bradbury and Baeyens (1998) suggest a relatively simple correction for the Opalinus Clay based on the dominant aqueous speciation to associate  $\text{Na}^+$  with  $\text{Cl}^-$  measured in the aqueous extracts, and  $\text{SO}_4^{2-}$  with  $\text{Ca}^{2+}$ . The sulphate correction could be further refined to account for any  $\text{Mg-SO}_4$  and  $\text{Na-SO}_4$  complexation, and to compensate for the cations charge-balancing the extra-alkalinity generated from calcite dissolution. Chloride carries 90% of the anion charge in normal Opalinus Clay pore water, and sodium 80% of the cation charge. Note that the source of sulphate in the aqueous extracts appears to be dominantly mineral dissolution (+/- minor pyrite oxidation / calcite dissolution) and therefore the counter-ions associated with extra sulphate are not primarily pore water components but more likely  $\text{Ca}^{2+}$ . Corrections were therefore made by subtracting an amount of  $\text{Na}^+$  equivalent to  $\text{Cl}^-$  in the aqueous extract and an amount of  $\text{Ca}^{2+}$  equivalent to  $\text{SO}_4^{2-}$ .

The measured CEC, as the sum of the exchangeable cations, ranges from 10.4-11.6 meq/100g for all samples applying corrections as discussed above. (Fig. 11). The Ni consumption balances the CEC within the analytical uncertainties.

The fractional cation occupancies on the exchanger ( $X_i$ ) were calculated (Table 4) according to  $X_i = C_i / CEC$ , where  $C_i$  is the quantity of cation in milli-equivalents ( $Na^+$ ,  $K^+$ ,  $Mg^{2+}$ ,  $Ca^{2+}$ ,  $Sr^{2+}$ ) on the permanent charge sites after corrections, and CEC is the sum of exchangeable cations.

#### 5.4. Stable isotope composition of carbonates and pore water

$\delta^{13}C$  and  $\delta^{18}O$  of calcite along profile A vary between -0.6 and -0.4 ‰ PDB, and between +24.8 and +25.1 ‰ VSMOW, respectively (Fig. 12). The isotopic variations cover the same range as the analytical error. Moreover,  $\delta^{13}C$  and  $\delta^{18}O$  of calcite measured at the end of the experiment are quite similar to  $\delta^{13}C$  and  $\delta^{18}O$  of calcite previously analysed in the initial borehole at the same depth:  $\delta^{13}C = -0.2$  ‰ and  $\delta^{18}O = +25.0$  ‰ (Gaucher et al., 2002). In contrast, calcite at the water/rock interface of the PC-borehole with a  $\delta^{13}C$  of -1 ‰ and a  $\delta^{18}O$  of +23.1 ‰ is significantly  $^{18}O$ -depleted relative to the calcite in the Opalinus clay.

The  $\delta^{18}O$  values of pore water obtained from the isotope diffusive-exchange method range from -7.46 ‰ to -8.20 ‰ for a five-point profile at level C without showing a gradient (data not given). Cumulative errors range from  $\pm 0.35$  ‰ to  $\pm 1.1$  ‰ for the individual experiments. Due to one failed experiment (leaky container), only a three-point profile is available for level B, ranging from -6.38 ‰ to -8.55 ‰, showing more scatter but no trend. The  $\delta^2H$  values range from -36.7 ‰ to -66.6 ‰ for profile C defining a near-linear gradient (Fig. 13), but are inconclusive for the partial profile at level B. The full data set is given in Koroleva and Mäder (2008).

## 6. Discussion

### 6.1. Water content and density

The water content does not vary significantly along radial profiles (Fig. ). However, the value is highest in the sample adjacent to the PC-borehole and lowest at the outer rim.

This is likely an effect of a disturbed zone with a slightly higher porosity surrounding the test interval. The water content values obtained by drying of the rock material after the isotope diffusive-exchange experiment as well as the calculated water content from isotopic composition show the same decreasing trend away from the borehole. This may be attributed to some swelling effects. Nevertheless, the physical properties are rather uniform and do not vary by much that could be related to water-rock interaction processes. Even bulk wet densities are not significantly lower or higher adjacent to the test interval (Fig. ) where the most prominent changes might be expected.

#### 6.2. Gradients in pore water composition

Due to electrostatic repulsion at negatively charged clay surfaces, porosity accessible to anions is lower than for water or cations in claystones. Comparison of  $\text{Cl}^-$  and  $\text{Br}^-$  data in aqueous extract solutions with those in the test interval present for the last 300 days ( $\text{Cl}^- \approx 276$  mmol/kg<sub>H<sub>2</sub>O</sub>,  $\text{Br}^- \approx 3.97$  mmol/kg<sub>H<sub>2</sub>O</sub>, Table 1) shows that the anion accessible porosity is approximately 75% of the total porosity. Previous measurements at Mont Terri yielded ratios of chloride porosity to the water-loss porosity of  $\sim 0.6$  with a range of reliable values from 0.5 to 0.7 (Pearson 1999; Pearson *et al.*, 2003 Fig. A10.8). Measurements of diffusion of both water (measured using HTO) and chloride have also been made on several samples from Mont Terri. The ratio of the diffusion porosity for chloride to that of HTO is also between 0.5 and 0.7 (Pearson *et al.*, 2003, Table A10.8; Van Loon *et al.*, 2003, 2004). As a consequence, the value obtained from the overcore samples is the highest reliable value measured on Opalinus clay samples. The reason for this high value could not be correlated to any rock parameter but may be due to some relaxation effect close to the borehole affecting the clay micro fabric but not bulk properties. There was a small annular gap of 1 mm present initially when the equipment was inserted into the open borehole, and this gap did close during the experiment implying some relaxation.

While Cl concentration in the test interval was very similar to the in-situ Cl concentration in the porewater, Br concentration was much higher in the test interval than in the formation. As a consequence, Cl and Br concentration profiles (Fig. 9) are in agreement with what is expected from a diffusion process (see Tournassat et al., 2010, this issue, for modelling details). The Br/Cl molal ratio obtained at 17 cm distance ( $6 \cdot 10^{-3}$ ) is still higher than the one typically observed for the Opalinus Clay formation at Mont Terri (Br/Cl ratio  $\sim 3 \cdot 10^{-3}$ , Pearson et al., 2003). This indicates that the diffusion profile is extending beyond 17 cm.

In contrast to Cl and Br, the sulphate concentrations in pore water calculated from aqueous leachates are significantly higher than those observed in the test interval. Sub-samples located adjacent to the test interval yield a recalculated sulphate concentration in pore water of 27 mmol/kg<sub>H<sub>2</sub>O</sub> (liquid nitrogen preservation, 10-minute extract) and 33-40 mmol/kg<sub>H<sub>2</sub>O</sub> (vacuum-sealed, 7-day extract), but the test interval contains only 4.6 mmol/kg<sub>H<sub>2</sub>O</sub> at the end of the field experiment (Fig. 10, Table 1). Samples at the far end of the profile yield 45-63 mmol/kg<sub>H<sub>2</sub>O</sub> SO<sub>4</sub><sup>2-</sup> which is a factor of 3-4 higher than the expected value of ca. 15 mmol/kg<sub>H<sub>2</sub>O</sub> used for the initial pore water composition (Table 1). It is concluded that there must be either (1) a significant amount of dissolution of a soluble sulphate mineral during the aqueous leaching test, or (2) a slight oxidation of the sample material (e.g., pyrite, or secondary sulphides). Gaucher et al. (2009) observed extracted sulphate values that were three times too high compared to pore water for Callovian-Oxfordian claystone from Bure, France, and explained this by celestite dissolution during the extractions. Here, the good agreement between extractions performed at 10 minutes, 24 hours and 7 days do not indicate the presence of celestite. Secondary sulphides similar to those described from the borehole interface may have formed due to the increasing in-diffusion of dissolved sulphide following its concentration increase in the test interval. Although the sample preservation methods chosen were previously shown to prevent oxidation of pre-existing pyrite (Pearson et al.,

2003; Gaucher et al., 2009), newly-formed Fe-sulphides may be more labile and are likely more difficult to preserve. Partial oxidation of the sample (pyrite, other Fe-sulphides) can therefore not be excluded. The oxidation of less than 0.2 g of pyrite per kg of rock is sufficient for explaining the observed discrepancies, i.e. approximately 1% of the total pyrite content of the sample. These results confirm that it is very difficult to obtain reliable sulphate concentrations from leaching experiments of core samples due to side reactions that are very difficult to prevent completely. Despite these limitations, a sulphate gradient can be observed in the data. Although recalculated concentration values are not consistent with concentrations in the test water, the gradient is in accord with the substantial reduction in sulphate concentrations over time in the test interval, from near 15 to 4-5 mmol/kg, leading to a strong gradient and associated flux of sulphate towards the test interval.

The artificial pore water was initially traced for a large positive  $\delta^2\text{H}$  of +370 ‰, and  $\delta^{18}\text{O}$  was at a laboratory water value of -10.46 ‰. The final sampling campaign (17 days before overcoring) yielded values of -13 ‰ and -5.93 ‰ for  $\delta^2\text{H}$  and  $\delta^{18}\text{O}$ , respectively. Slow but continuous in-flow of pore water occurred to the interval after final sampling, and this may have affected especially the  $\delta^2\text{H}$  profile.  $\delta^{18}\text{O}$  values show no variation with radial distance for the profile at 9.7 m depth (C) with an average of -7.8 ‰ (range: -7.5 to -8.2 ‰). This range is partially overlapping with values obtained by the same method from a nearby borehole BWS-A2 (1 sample, -7.7 ‰) and a somewhat more distant borehole BWS-A5 (9 samples, crossing Main Fault, -7.1 ‰ to -7.6 ‰) reported in Pearson et al. (2003, Table A4.3). Values around -9.0 ‰ measured in the inflow from long-term pore water sampling in BWS-A2 appear enigmatic and the discrepancy remains unexplained (Pearson et al., 2003, Table A1.14). Data therefore suggest that the  $\delta^{18}\text{O}$  remained largely undisturbed in the rock matrix during the PC experiment.

In contrast,  $\delta^2\text{H}$  (Fig. 13, profile at 9.5 m depth) shows an approximately regular decrease from -36 ‰ near the borehole to -67 ‰ at a radial distance of ca. 15 cm measured

along bedding. This latter value is consistent with values of -59 ‰ to -66 ‰ measured on the inflow in a borehole at a similar structural position (Pearson et al. 2003, borehole BWS-A2, Table A1-14), but more negative than a value obtained from core material from the same borehole by diffusive exchange (Pearson et al. 2003, Table A4-3). While this latter discrepancy between different methods remains unclear, the profile obtained for deuterium is in agreement, like those for Cl and Br, with diffusion processes having taken place during the five years of the experiment. The pattern obtained for a four-sample profile at 6.7 m depth is less clear due to the fact that one experiment apparently leaked as documented by an erroneously high apparent water content.

The combined oxygen and hydrogen data of the test porewater monitored during five-years and of the Opalinus clay overcored at the water/rock interface were plotted in a  $\delta^{18}\text{O}$  –  $\delta^2\text{H}$  diagram (Fig. 14). The figure shows the slight  $^2\text{H}$  diffusion into the Opalinus clay and the strong buffering of the Opalinus clay formation.

### *6.3. Stability of the clay exchanger and of the mineral assemblage*

Fig. 11 illustrates the cation occupancies on the exchanger as a function of radial distance from the borehole. For all samples the occupancy is approximately 5.5 meq/100g for  $\text{Na}^+$ , 2.2 meq/100g for  $\text{Ca}^{2+}$ , 2.0 meq/100g for  $\text{Mg}^{2+}$ , approximately 0.8 meq/100g for  $\text{K}^+$ , and the  $\text{Sr}^{2+}$  data shows a very narrow spread at a value of 0.13 meq/100g. The fractional cation occupancies on the exchanger are therefore identical in all investigated samples. Furthermore, the data obtained for the profiles compare rather well with undisturbed Opalinus Clay reported in Pearson et al. (2003, Tab. A3.11) for the locations in a comparable position (BWS-A3) and obtained by a comparable Ni-en method with similar corrections applied: 9.5-10.4 meq/100g for the sum of exchangeable cations, 4.8-5.0 meq/100g for  $\text{Na}^+$ , 2.5-2.7 meq/100g for  $\text{Ca}^{2+}$ , 1.6-1.9 meq/100g for  $\text{Mg}^{2+}$ , and ca. 0.1 meq/100g for  $\text{Sr}^{2+}$ . The occupancy

obtained in BWS-A3 for  $K^+$  (0.5-0.7 meq/100g) is somewhat less than the value obtained from the PC samples.

The mineralogy of the mud collected on the wall of the borehole and precipitates in the borehole fluid provide evidence of neoformations of Fe-bearing sulphides (pyrite, and probably greigite and/or mackinawite) and calcite, induced by the microbial perturbation (Wersin et al., 2010a, b; this issue; Stroes-Gascoyne et al., 2010; this issue; Tournassat et al., 2010; this issue). A source of  $Fe^{2+}$  is required for this Fe-bearing mineral precipitation.  $Fe^{2+}$  originates ultimately from the formation pore water by diffusion (neither initial test water nor equipment devices did contain Fe). In the formation,  $Fe^{2+}$  can originate from the clay exchanger (Tournassat et al., 2009; Pearson et al., 2010; this issue) or from a dissolving solid phase (pyrite, siderite, clay minerals or detrital phases such as biotite, Pearson et al., 2003). There was, however, no notable decrease in siderite towards the test interval. Pyrite dissolution is not possible from a thermodynamic and mass balance point of view: first, the bacterial perturbation led to more reducing conditions than those present in-situ (Pearson et al., 2010; this issue) and second, the stoichiometric dissolution of pyrite would produce one Fe for two S while precipitation of the observed Fe-sulphides required more than one Fe atom for two S atoms. As a consequence, Fe in pore water (Table 1) and Fe from the exchanger are the most likely sources.

The  $^{18}O$  depletion in calcite in the mud collected from the wall of the borehole could be due to water/calcite isotopic exchange or precipitation of calcite from the borehole water. The  $\delta^{13}C$  and  $\delta^{18}O$  of the fluid at equilibrium with the calcite of the mud was calculated using the calcite-water oxygen isotope fractionation of O'Neil et al. (1969) and the calcite- $HCO_3^-$  carbon isotope fractionation of Deines et al. (1974), and a formation temperature between 15 and 25°C, i.e. the maximum range of temperatures measured in the borehole during the PC experiment. Calculated equilibrium  $\delta^{13}C$  and  $\delta^{18}O$  of ca. -3 ‰ PDB and ca. -7 to -5 ‰ VSMOW, respectively, are significantly different from the observed isotopic signature of the

initially injected synthetic porewater ( $\delta^{13}\text{C}$  and  $\delta^{18}\text{O}$  of -29.1 ‰ and -10.5 ‰, respectively). But the calculated isotopic composition is quite close to the pore water after 264 days. This is after major changes of the chemical parameters of the borehole water occurred as a consequence of bacterial perturbations (sulphate reduction), and the observed carbonates are inferred to have formed as a consequence of this.

Mineralogical, textural and chemical variations of bulk rock as well as of the clay fraction and (C, O) isotopes of carbonates along the radial profiles are small and may be considered as representative of the heterogeneity of the rock. Euhedral grains of carbonates (calcite, dolomite and siderite) at the water/rock interface do not provide any evidence of surface dissolution or growth. Pyrite framboids and clusters remained also stable. There is no visible evidence of precipitation/dissolution processes which could be linked to the effects of water-rock interaction during the PC experiment in the Opalinus clay adjacent to the test interval.

## 7. Conclusions

Mineralogical, chemical and isotopic analyses were performed on samples from overcoring a five-year in-situ diffusion experiment carried out in Opalinus Clay, and that was microbially disturbed. No mineralogical, chemical, physical and isotopic changes were observed in the Opalinus Clay bulk rock except for the immediate interfacial region and a very slight increase in water content next to the test interval. This is despite that the sulphate-sulphide system was heavily perturbed in the test interval.

Results show that the distribution of non-reactive tracers ( $\text{Br}^-$  and  $^2\text{H}$ ) in pore water display clear radial diffusion profiles and follows the expected out/in-diffusion compatible with the time-dependent boundary conditions in the borehole. Bromide concentration decreases with distance from the test interval, and thus also Br/Cl ratios. The Br/Cl ratio does not reach a plateau in the range of 0-17 cm.

The determined apparent anion-accessible porosity ratio of ~0.75 is slightly higher than the range of 0.5-0.7 of existing data. It is not clear if this is due to a physico-chemical disturbance induced by the experiment.

In summary, only very minor effects in the wall rock resulted from a five-year microbially perturbed in-situ test (sulphate reduction and oxidation of organic carbon). This attests to the expected relatively rapid buffering processes and large buffering capacity of Opalinus Clay provided by its mineralogy and ion exchange complex.

### **Acknowledgements**

Financial support by the partners of the Mont Terri Consortium participating in the PC Experiment (ANDRA, BGR, CRIEPI, JAEA, Nagra, SCK-CEN) is acknowledged. The support of field work by Christophe Nussbaum and Thierry Theurillat (Geotechnical Institut AG / Swisstopo) and the excellent drilling work supported by Bernd Frieg (Nagra) and carried out by Schützeichel Kernbohrergesellschaft is highly appreciated. Chr. Tournassat (BRGM) and F.J. Pearson (New Bern, consultant) provided a review of an earlier version. E. Sacchi (Università di Pavia) and an anonymous reviewer improved clarity of arguments and presentation.

### **References**

- Bradbury, M.H., Baeyens, B., 1998. A physicochemical characterization and geochemical modeling approach for determining porewater chemistries in argillaceous rocks. *Geochim. Cosmochim. Acta* 62, 783-795.
- De Cannière, P., Schwarzbauer, J., Höhener, P., Lorenz, G., Salah, S., 2011. Biogeochemical processes in a clay formation in-situ experiment: Part C - Organic contamination and leaching data. *Applied Geochemistry* (this issue).

- Deines, P., Langmuir, D., Harmon, R.S., 1974. Stable carbon isotope ratios and the existence of a gas phase in the evolution of carbonate groundwaters. *Geochim. Cosmochim. Acta* 38, 1147-1164.
- Gaucher E.C., Crouzet C., Flehoc C., Girard J.P., Lassin A., 2002. Measurement of partial pressure and isotopic composition of CO<sub>2</sub> on two core samples from the Mont Terri Rock Laboratory, borehole BPC-1. Report BRGM/RP-51771-FR, BRGM, France.
- Gaucher, E. C., Tournassat, C., Pearson, F. J., Blanc, P., Crouzet, C., Lerouge, C., Altmann, S., 2009. A robust model for clayrock porewater chemistry. *Geochim. Cosmochim. Acta* 73, 6470-6483.
- Gimmi, T., 2003. Porosity, pore structure, and energy state of pore water of Opalinus Clay from Benken. Nagra Internal Report NIB 93-09, Nagra, Wettingen, Switzerland.
- Horita, J., Cole, D.R., Wesolowski, D.J., 1993a. The activity-composition relationship of oxygen and hydrogen isotopes in aqueous salt solutions: II. Vapor-liquid water equilibration of mixed salt solutions from 50 to 100°C and geochemical implications. *Geochim. Cosmochim. Acta* 57, 4703-4711.
- Horita, J., Wesolowski, D.J., Cole, D.R., 1993b. The activity-composition relationship of oxygen and hydrogen isotopes in aqueous salt solutions: I. vapor-liquid water equilibration of single salt solutions from 50 to 100°C. *Geochim. Cosmochim. Acta* 57, 2797-2817.
- Koroleva, M., Mäder, U., 2008. PC-Experiment: Geochemical analysis of sample material from overcoring BPC-1. Mont Terri Project, Technical Note 2006-68.
- NAGRA, 2002. Projekt Opalinuston: Synthese der geowissenschaftlichen Untersuchungsergebnisse. Entsorgungsnachweis für abgebrannte Brennelemente, verglaste hochaktive sowie langlebig-mittelaktive Abfälle. Nagra Technical Report NTB 02-03, Nagra, Wettingen, Switzerland.

- O'Neil, J.R., Clayton, R.N., Mayeda, T.K., 1969. Oxygen isotope fractionation in divalent metal carbonates. *J. Chem. Phys.* 51, 5547-5558.
- Pearson, F. J., 1999. What is the porosity of a mudrock? In: Aplin, A. C., Fleet, A. J., Macquaker, J. H. S. (Eds.), *Muds and Mudstones: Physical and Fluid Flow Properties*. Geol. Soc. London Spec. Pub. 158, 9-21.
- Pearson, F.J., Arcos, D., Bath, A., Boisson, J.Y., Fernandez, A.M., Gaebler, H.E., Gaucher, E.C., Gautschi, A., Griffault, L., Hernan, P., Waber, H.N., 2003. Mont Terri Project – Geochemistry of Water in the Opalinus Clay Formation at the Mont Terri Rock Laboratory. Reports of the Federal Office of Water and Geology (FOWG), Geology Series No. 5.
- Pearson, F.J., Tournassat, C., Gaucher, E., 2011. Biogeochemical processes in a clay formation in-situ experiment: Part E - Equilibrium controls on chemistry of pore water from the Opalinus Clay, Mont Terri Underground Laboratory, Switzerland. *Applied Geochemistry* (this issue).
- Rübel, A., Sonntag, Ch., Lippmann, J., Pearson, F.J., Gautschi, A., 2002. Solute transport in formations of very low permeability; profiles of stable isotope and dissolved noble gas contents of pore water in the Opalinus Clay, Mont Terri, Switzerland. *Geochim. Cosmochim. Acta* 66, 1311-1321.
- Soler, J.M., Samper, J., Yllera, A., Hernández, A., Quejido, A., Fernández, M., Yang, C., Naves, A., Hernán, P., Wersin, P., 2008. The DI-B in situ diffusion experiment at Mont Terri: Results and modelling. *Phys. Chem. Earth* 33, 196–207.
- Sposito G., 1990. Molecular Models of Ion Adsorption on Mineral Surfaces. In: Hochella, M.F., White, A.F. (Eds.). *Mineral-Water Interface Geochemistry*. Min. Soc. America, *Reviews in Mineralogy* 23, 261-279.

- Swart P.K., Burns S.J., Leder J.J., 1991. Fractionation of the stable isotopes of oxygen and carbon in carbon dioxide during the reaction of calcite with phosphoric acid as a function of temperature and technique. *Chem. Geol.* 86, 89-96.
- Stroes-Gascoyne, S., Sergeant, C., Schippers, A., Hamon, C.J., Nèble, S., Vesvres, M.-H., Barsotti, V., Poulain, S., Le Marrec, C., 2011. Biogeochemical processes in a clay formation in-situ experiment: Part D - Microbial analyses - synthesis of results. *Applied Geochemistry* (this issue).
- Tournassat, C., Gailhanou, H., Crouzet, C., Braibant, G., Gautier, A., and Gaucher, E. C., 2009. Cation exchange selectivity coefficient values on smectite and mixed-layer illite/smectite minerals. *Soil Sci. Soc. Am. J.* 73, 928-942.
- Tournassat, C., Alt-Epping, P., Gaucher, E.C., Gimmi, T., Leupin, O.X., Wersin, P., 2011. Biogeochemical processes in a clay formation in-situ experiment: Part F - Reactive transport modelling. *Applied Geochemistry* (this issue).
- Van Loon, L. R., Soler, J. M., Jakob, A., Bradbury, M. H., 2003. Effect of confining pressure on the diffusion of HTO,  $^{36}\text{Cl}^-$  and  $^{125}\text{T}$  in a layered argillaceous rock (Opalinus Clay): diffusion perpendicular to the fabric. *Appl. Geochem.* 18, 1653-1662.
- Van Loon, L. R., Soler, J. M., Muller, W., Bradbury, M. H., 2004. Anisotropic diffusion in layered argillaceous rocks: a case study with Opalinus Clay. *Environ. Sci. Technol.* 38, 5721-5728.
- Wersin, P., Gaucher, E., Gimmi, Th., Leupin, O., Mäder, U., Pearson, F.J., Thoenen, T., Tournassat, Ch., 2009. Geochemistry of pore waters in Opalinus Clay at Mont Terri: experimental data and modelling. Mont Terri Project, Technical Report 2008-06.
- Wersin, P., Leupin, O.X., Mettler, S., Gaucher, E., Mäder, U., Vinsot, A., De Cannière, P., Gäbler, H.-E., Kunimaro, T., Kiho, K., 2010a. Biogeochemical processes in a clay formation in-situ experiment: Part A - Overview, experimental design and water data. *Applied Geochemistry* (this issue).

Wersin, P., Stroes-Gascoyne, S., Pearson, F.J., Tournassat, C., Leupin, O.X., Schwyn, B.,  
2010b. Biogeochemical Processes in a Clay Formation In-situ Experiment: Part G –  
Key interpretations & conclusions. Implications for repository safety. Applied  
Geochemistry (this issue).

Formatted: English (United Kingdom)

**Table 1** Concentrations (mmol/L) in the test interval for select parameters at initial time and at the final stage of the PC experiment (Wersin et al., this issue).

Sample name	Test water	PC-8	PC-9	PC-10	PC-12
Day after injection	0	1061	1316	1517	1846
pH (in line)	7.74	6.81	7.16	6.75	6.82
Eh (in line) mV SHE		-257	-275	-240	-250
Sodium	255	265	247	252	243
Potassium	1.5	2.0	2.0	2.1	1.8
Magnesium	18.0	18.3	18.1	19.5	17.1
Calcium	15.9	14.9	14.0	15.5	13.5
Iron	0.0023	0.1021	0.0290	0.0089	0.0030
Chloride	262	313	293	299	281
Bromide	29.4	3.3	3.5	3.8	4.0
Sulphate	14.7	4.3	4.1	5.0	4.3
Total sulphides	0	0.246	0.044	0.075	
Alkalinity	1.0	10.6	10.9	8.5	10.4
DOC/TOC	0.2	4.1	1.0	1.2	1.3
Methane	1e-4	0.12	0.72	0.25	0.084
$\delta^2\text{H} \text{‰}$	+370.0		-37	-32.7	-12.8
$\delta^{13}\text{C-DIC} \text{‰}$	-29.1		-12.3	-9.0	-11.5

**Table 2**

Aqueous leaching data at different S:L ratios, with concentrations scaled to dry rock mass.

Radial Distance (average) (cm)	Segment Depth (m)	Profile ID	S:L Ratio	Time of shaking (h)	Number of measure ments	Cl <sup>-</sup> (mmol/kg <sub>r</sub> )	Br <sup>-</sup> (mmol/kg <sub>r</sub> )	SO <sub>4</sub> <sup>2-</sup> (mmol/kg <sub>r</sub> )
0.5	6.5	A	0.001	0.1	3	19.8	<0.002	<0.003
0.5	6.5	A	0.01	0.1	3	16.6	0.21	1.50
0.5	6.5	A	0.10	0.1	8	16.8	0.20	1.55
0.5	6.5	A	0.10	24	5	17.8	0.20	1.65
1.5	6.7	B	0.10	168	1	16.0	0.15	2.28
1.5	6.7	B	0.25	168	1	16.0	0.17	2.28
1.5	6.7	B	0.50	168	1	16.3	0.18	2.27
1.5	6.7	B	1.00	168	1	17.0	0.19	1.89
1.6	6.5	A	0.10	0.1	1	14.6	0.17	1.43
1.6	6.5	A	0.10	24	1	15.0	0.16	1.57
2.8	6.5	A	0.10	0.1	3	14.7	0.17	1.45
2.8	6.5	A	0.06	24	1	15.2	0.17	1.59
2.8	6.5	A	0.10	24	1	15.3	0.17	1.59
2.8	6.5	A	0.09	24	1	17.1	0.20	1.85
3.8	6.5	A	0.10	0.1	1	14.8	0.17	1.60
3.8	6.5	A	0.10	24	1	15.2	0.17	1.66
4.8	6.5	A	0.10	0.1	1	14.4	0.16	2.29
4.8	6.5	A	0.10	24	1	14.8	0.16	2.35
5	6.7	B	0.10	168	2	15.2	0.12	2.27
5	6.7	B	0.25	168	2	15.1	0.15	2.33
5	6.7	B	0.50	168	2	15.5	0.16	2.32
5	6.7	B	1.00	168	2	16.2	0.16	2.21
6	6.5	A	0.10	0.1	1	14.4	0.15	2.00
6	6.5	A	0.10	24	1	14.4	0.15	2.06
7.8	6.5	A	0.10	0.1	3	14.1	0.13	2.95
7.8	6.5	A	0.10	24	1	14.2	0.13	4.75
9	6.7	B	0.10	168	2	15.6	<0.01	2.67
9	6.7	B	0.25	168	2	15.1	0.11	2.68
9	6.7	B	0.50	168	2	15.5	0.14	2.66
9	6.7	B	1.00	168	2	16.2	0.13	2.59
9.5	6.5	A	0.10	0.1	1	13.6	0.11	2.27
9.5	6.5	A	0.10	24	1	14.0	0.11	2.38
11.1	6.5	A	0.10	0.1	1	12.8	0.09	2.13
11.1	6.5	A	0.10	24	1	12.8	0.09	2.35
12.9	6.5	A	0.10	0.1	1	12.4	0.08	2.27
12.9	6.5	A	0.10	24	1	12.5	0.08	2.46
13	6.7	B	0.10	168	2	15.1	<0.01	2.74
13	6.7	B	0.25	168	2	14.7	0.09	2.83
13	6.7	B	0.50	168	2	15.1	0.12	2.79
13	6.7	B	1.00	168	2	15.8	0.11	2.70
14.7	6.5	A	0.10	0.1	3	13.3	0.08	3.11
14.7	6.5	A	0.10	24	3	13.4	0.08	4.73
16.8	6.5	A	0.001	0.1	3	16.7	<0.002	3.59
16.8	6.5	A	0.01	0.1	3	15.1	<0.002	2.69
16.8	6.5	A	0.10	0.1	3	14.7	0.08	2.52

**Table 3**

Ni-en extraction data at S:L ratio equal to 1 (Profile B) and CEC as sum of cations.

Radial Distance (average) (cm)	Ca <sup>2+</sup> (meq/100g)	Mg <sup>2+</sup> (meq/100g)	Na <sup>+</sup> (meq/100g)	K <sup>+</sup> (meq/100g)	Sr <sup>2+</sup> (meq/100g)	Sum of cations (meq/100g)	Ni <sup>2+</sup> (meq/100g)
1.5	2.6	2.0	7.2	0.8	0.13	12.8	10.5
5	2.7	1.9	7.1	0.8	0.12	12.7	10.7
9	2.8	1.9	7.0	0.8	0.13	12.5	10.8
13	2.8	1.9	7.0	0.8	0.13	12.6	10.9

**Table 4**

Fractional cation occupancies on the exchanger (Profile B).

Radial Distance (average) (cm)	X <sub>Ca</sub>	X <sub>Mg</sub>	X <sub>Na</sub>	X <sub>K</sub>	X <sub>Sr</sub>
1.5	0.21	0.19	0.51	0.08	0.012
5	0.21	0.18	0.52	0.08	0.012
9	0.22	0.18	0.52	0.07	0.012
13	0.21	0.18	0.52	0.08	0.012

## Figure captions

**Fig. 1.** Schematic of underground installation and excavation procedure, with exaggerated horizontal scale. (1) Auxiliary borehole (200 mm OD), (2) overcoring of service tube and resin infill, (3) overcoring of test interval (384 mm OD). See Wersin et al. (2010a, this issue) for details of surface installations.

**Fig. 2.** Scheme of the overcoring and sample locations, including profiles A, B and C, and two samples of black deposit scraped off the wall of the PC borehole.

**Fig. 3.** Distribution of the carbonate content as a function of distance (Profile A).

**Fig. 4.** Secondary electron (SE) image and corresponding (Fe, Si, Ca, S, K) elemental maps of the region within 300  $\mu\text{m}$  of the water/rock interface with interpreted mineral distribution. The morphology of the interface is visible on the SE image on the right. Combined K and Si maps show the homogeneous distribution of clay minerals at the interface. Combined Ca, Fe and S maps show the distribution of primary euhedral calcite, dolomite and siderite at the interface, but also the neoformation of a calcite, and the presence of gypsum close to the interface.

**Fig. 5.** Secondary electron images of primary minerals at the water/rock interface. a) pyrite close to the interface; b) dolomite crystal close to the interface; c) siderite in a relatively oriented clay matrix; d) microporosity with calcite neoformation; e, f) disorientation of clay minerals at the water/rock interface.

**Fig. 6.** X-ray diffraction pattern of mud collected in the borehole, compared with X-ray diffraction patterns of Opalinus clay samples of radial profile A.

**Fig. 7.** Back-scattered electron images and corresponding EDX spectra of sulphide and sulphate

phases in suspension in the water from the borehole. a) Fe-S sulphide phase with a Fe/S ratio ~1; b) Fe-S sulphide phase with a Fe/S ratio ~ 0.5; c) Ca-Na sulphate.

**Fig. 8.** Water content relative to dry mass and bulk wet density as function of distance (Profile B).

**Fig. 9.** Cl<sup>-</sup> and Br<sup>-</sup> in pore water and in the test interval as function of radial sample distance (Profiles A and B). Estimated errors are ± 10%.

**Fig. 10.** SO<sub>4</sub><sup>2-</sup> concentrations in pore water computed from aqueous leachates as function of radial sample distance (Profiles A and B), and coded for leaching duration and sample preservation technique (liquid nitrogen, sealed in vacuum).

**Fig. 11.** Cation occupancy as function of distance (Profile B).

**Fig. 12.** Carbon and oxygen isotopic composition of calcite as function of distance (Profile A).

**Fig. 13.** δ<sup>2</sup>H in pore water as function of radial sample distance (Profile C).

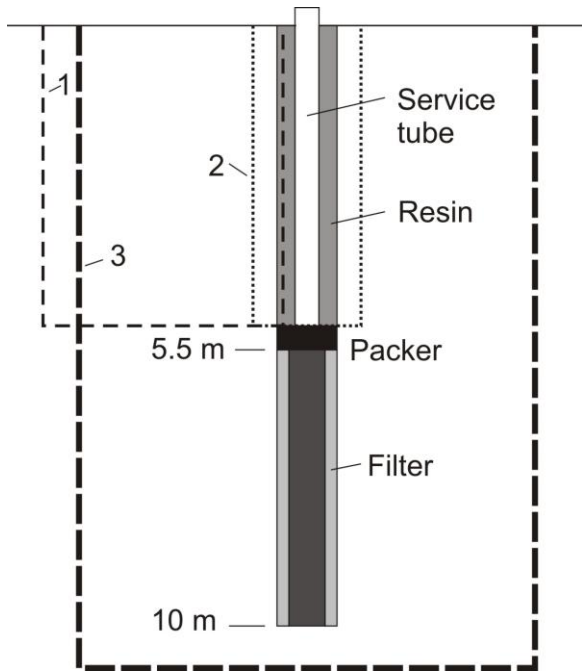


Fig. 1

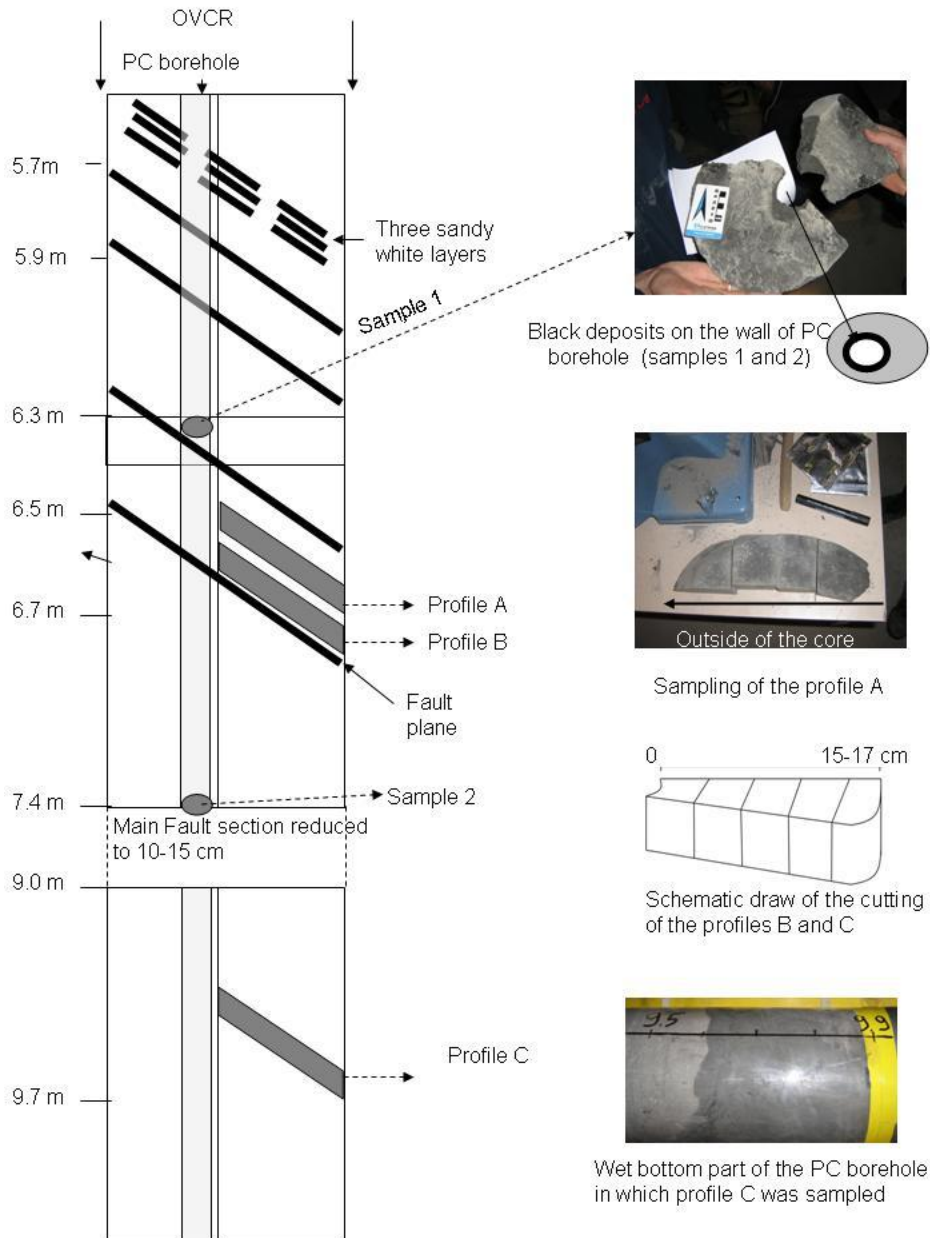


Fig. 2

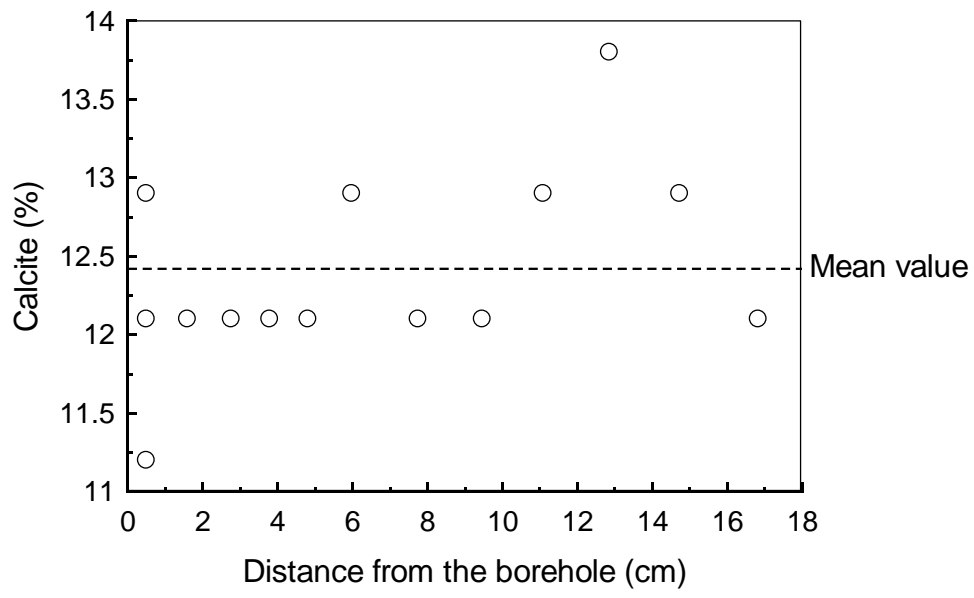


Fig. 3

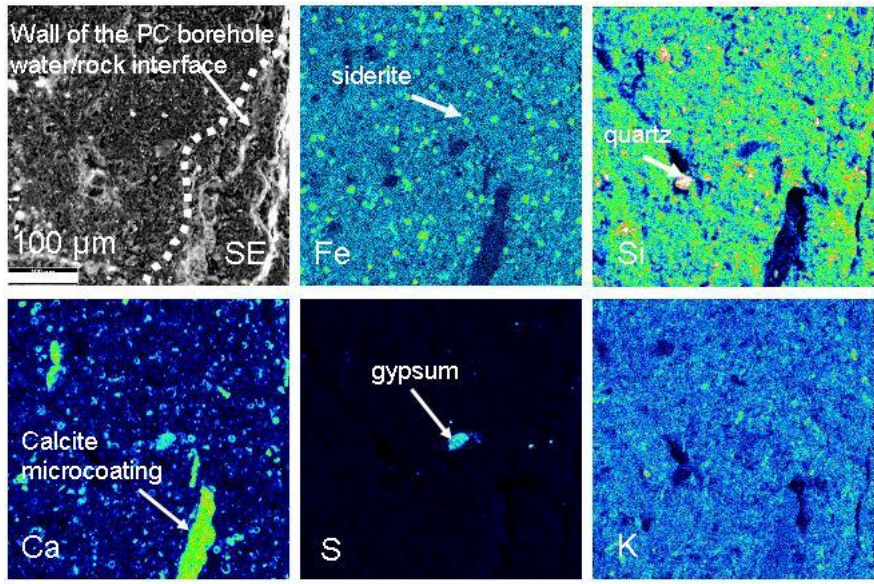
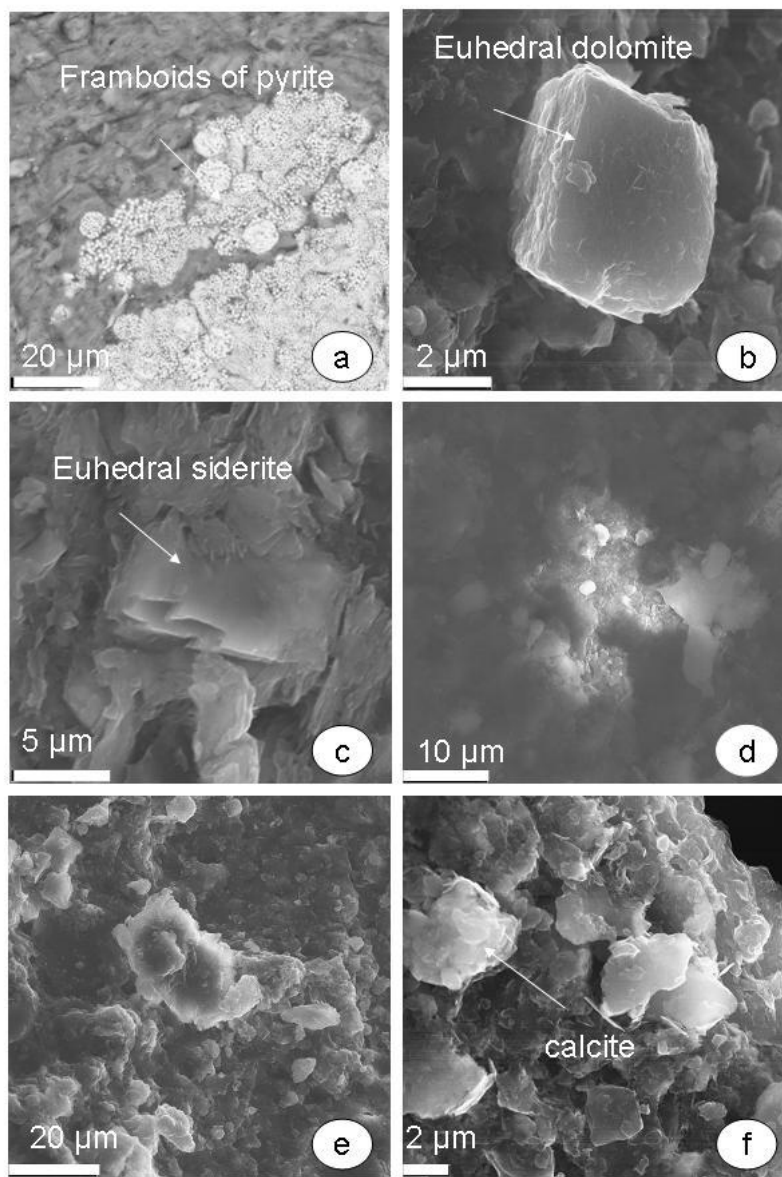


Fig. 4



**Fig. 5**

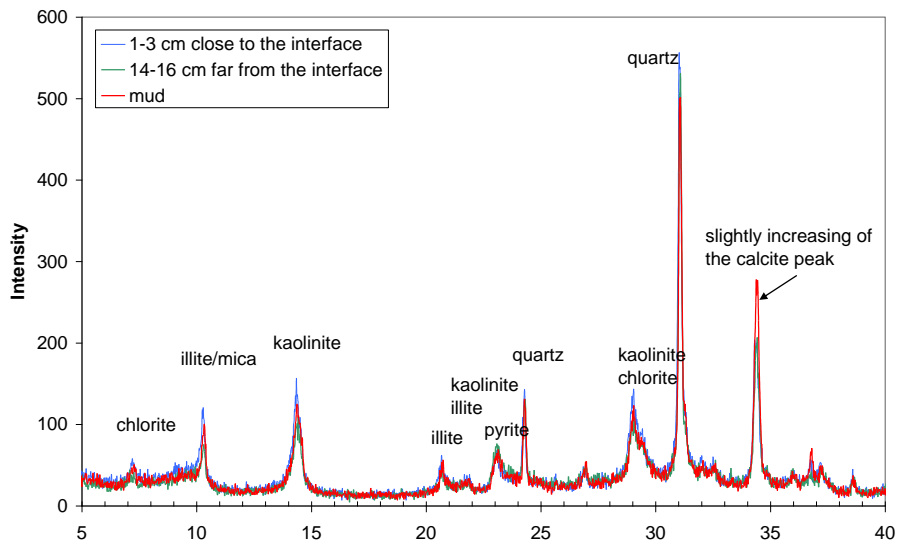


Fig. 6

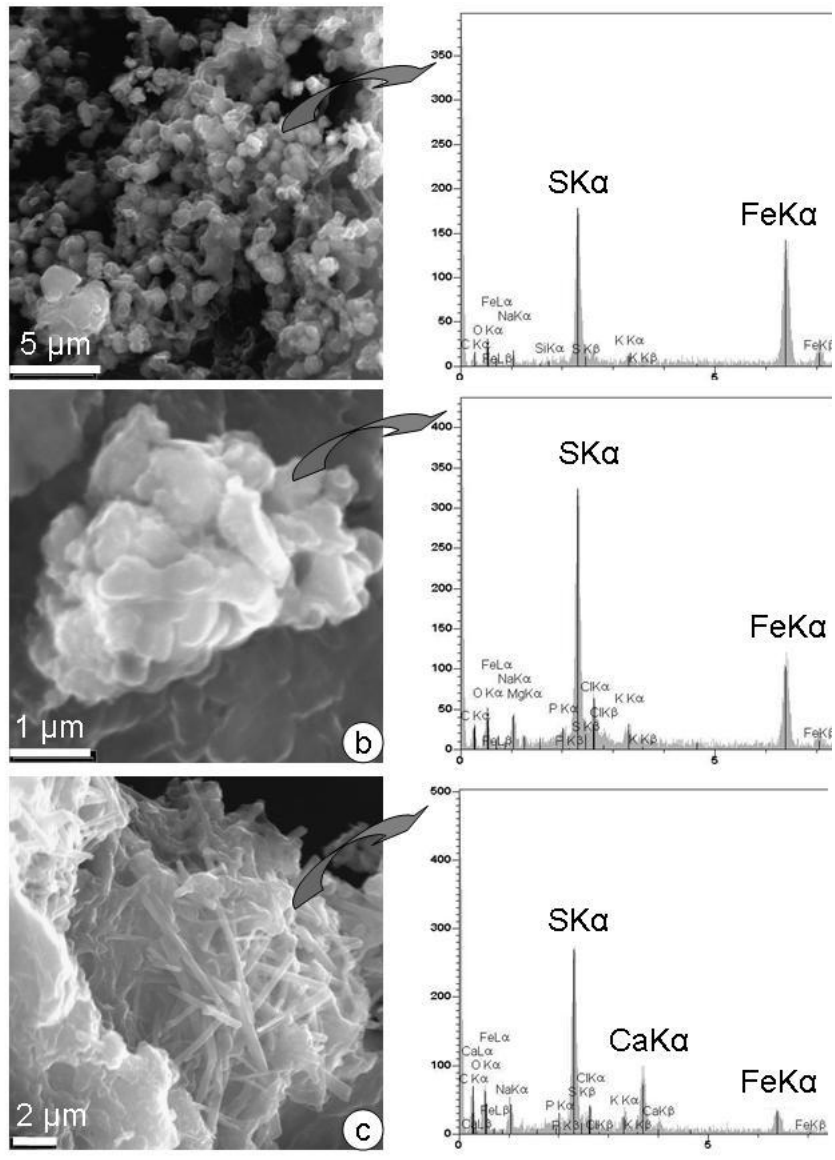


Fig. 7

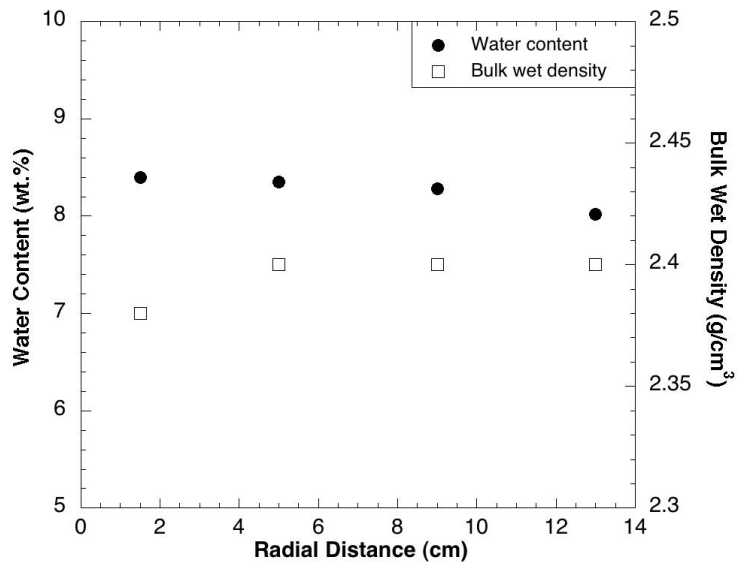


Fig. 8

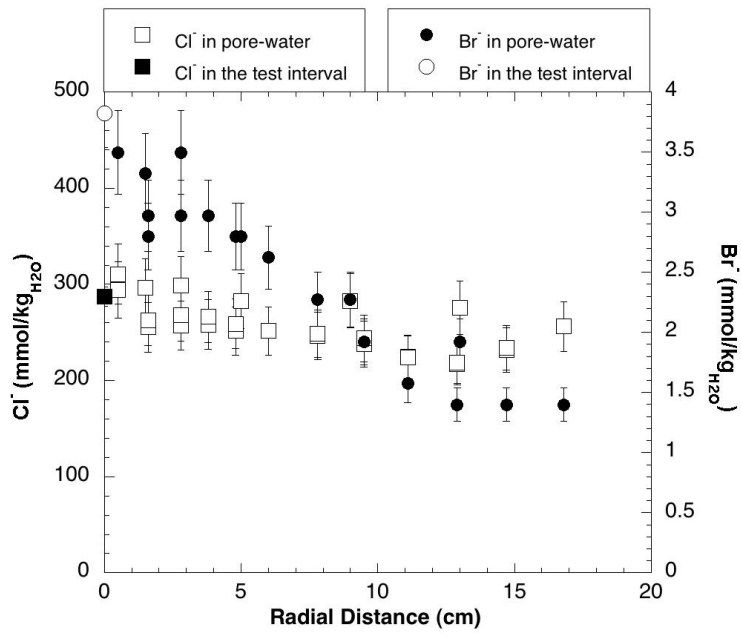


Fig. 9

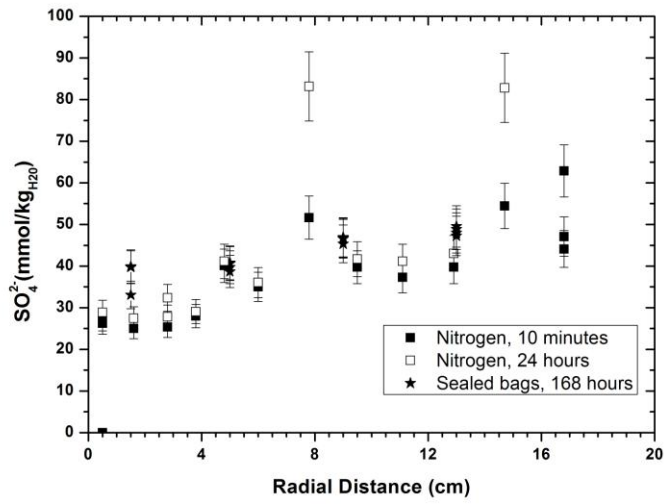


Fig. 10

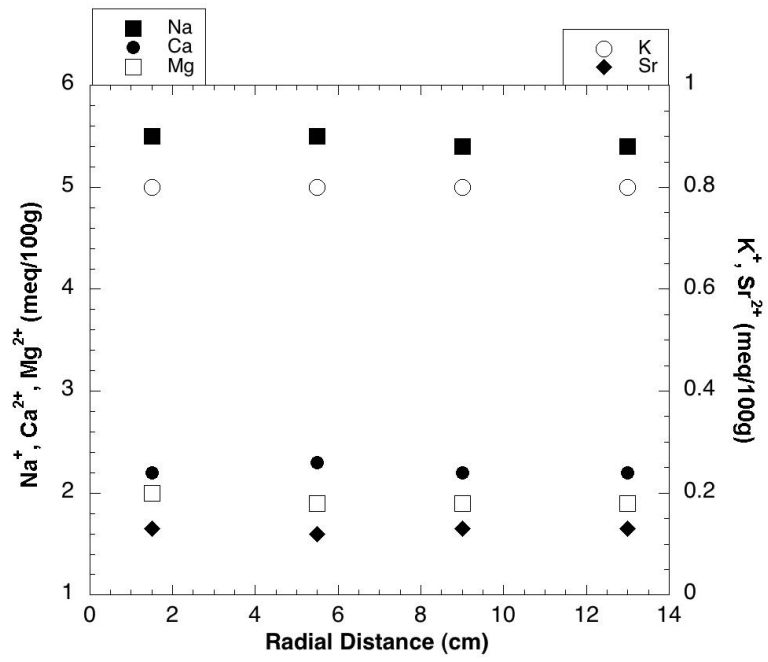


Fig. 11

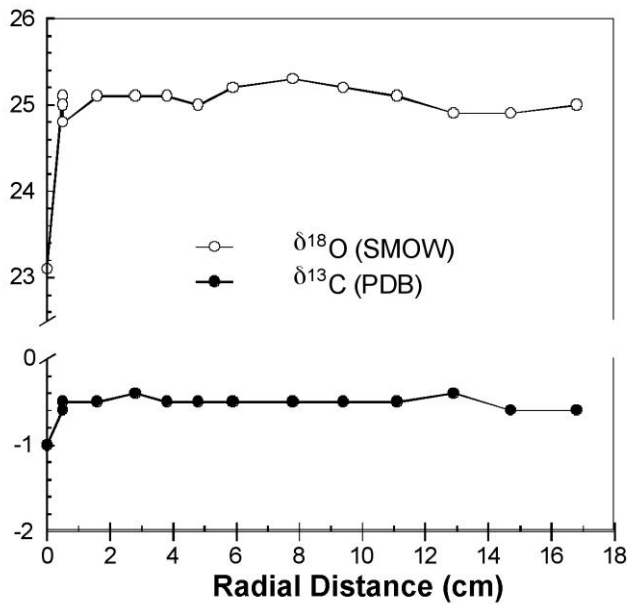


Fig. 12

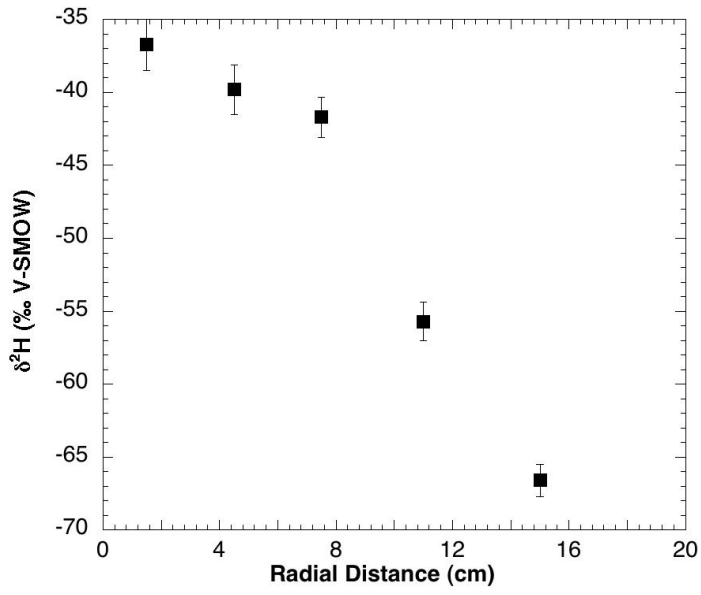


Fig. 13